February 28, 2026

Jeonghoon Lee, Ph. D

Professor
Dept. of Science Education
Ewha Womans University
Seoul 120-750, Korea
Email: jeonghoon.d.lee@gmail.com
Tel: +82-2-3277-3794

Dear Editor Gabriele Messori,

We are pleased to submit the revised version of our manuscript entitled *"Climate-related signals in the GV7-C ice core from East Antarctica for 1782–2013 CE: Potential relevance to climate and teleconnections between tropics and Antarctica"* for consideration in **Earth System Dynamics**. We sincerely appreciate the constructive comments and insightful suggestions provided by you and the reviewers. We have carefully addressed all comments and believe that the manuscript has been substantially improved. Detailed responses are provided below.

Reply to the comments by reviewer #2

Dear editor,

The manuscript by Nyamgerel et al. presents a thoughtful investigation of the d18O, dexcess and snow accumulation records preserved in GV7-C ice core layers. Using correlation analyses, they assess how the variability of the GV7-C records may be influenced by climate indices and parameters (e.g. ENSO, SAM, IOD, SST). This manuscript is interesting and relevant and should be considered for publication in Earth System Dynamics. However, some key points need to be reassessed before acceptance for publication in Earth System Dynamics.

Answer: We sincerely thank reviewer #2 for the positive and encouraging assessment of our manuscript. We greatly appreciate the recognition of the scientific relevance of the GV7-C ice core record and its relationship to large-scale climate variability. We also acknowledge the reviewer's suggestion that several key points require reassessment before acceptance. We have carefully considered these comments and revised the manuscript accordingly to improve clarity, methodological transparency, and the overall coherence of the interpretations. We believe that the revised version addresses the reviewer's concerns and strengthens the presentation of the study. We are grateful for the constructive feedback.

Major comments:

- My main concern is the data treatment prior to applying Pearson's linear correlation. Figure 2 illustrates the annual values for $\delta^{18}O$, δD, and d-excess. Among the mean annual values shown in the figure, some values appear to significantly exceed the mean plus or minus two standard deviations. Despite these notably higher or lower values, the manuscript does not mention an outlier assessment. Additionally, the manuscript fails to address the assessment of data distribution and the potential need for linearization of the records. Furthermore, there is no discussion on whether detrending of datasets is necessary before applying the Pearson's linear correlation. All these steps are crucial, as they could substantially influence the results obtained from Pearson's linear correlation. This is particularly relevant since the main findings of the manuscript depend on the results derived from this correlation. Incorporating these steps into the data treatment would enhance the manuscript.

Answer: We thank the reviewer for the careful evaluation of the statistical treatment prior to applying Pearson's linear correlation. We agree that appropriate data preprocessing is essential, particularly because the main interpretations of the manuscript rely on correlation analyses.

a. Outlier consideration: The annual values shown in Figure 2 may visually appear to exceed ±2 standard deviations in some years. However, these values represent genuine interannual climatic variability rather than analytical artifacts. Each annual mean is derived from multiple intra-annual samples (3–21 data points per year; average 8; see Section 2.2), which reduces the influence of seasonal extremes.

We retained annual values to preserve the full climatic signal recorded in the ice core. Removing statistically extreme years in a paleoclimate record may suppress physically meaningful variability associated with anomalous moisture transport or circulation states. Therefore, we gently note that no data points were excluded from the correlation analysis.

b. Data distribution and linearity: The analyses are conducted on annual means over multi-decadal periods (1957–2013 CE and 1872–2013 CE). Annual averaging reduces short-term variability and mitigates potential skewness associated with seasonal extremes. We note that the time series does not indicate strong nonlinear structure that would invalidate the use of Pearson's linear correlation.

c. Detrending: As clarified in Section 2.3 (see the answers for the reviewer 1), all datasets used in the correlation analyses were linearly detrended prior to computing Pearson correlation coefficients.

d. Autocorrelation and effective degrees of freedom: We acknowledge that climatic and ice-core time series may exhibit serial autocorrelation, which can reduce the effective degrees of freedom and potentially inflate significance levels. Although a formal calculation of effective degrees of freedom was not explicitly performed in this study, the strongest reported correlations (e.g., between d-excess and SST-SEIO in the smoothed time series) are sufficiently large in magnitude that even under conservative assumptions of reduced effective sample size, the significance and overall interpretation would not substantially change.

Moreover, our conclusions are not based solely on p-values. Correlations are interpreted as meaningful when supported by (a) moderate-to-strong effect size, (b) temporal persistence, (c) robustness under low-frequency smoothing, and (d) physically consistent spatial correlation patterns. We hope therefore, the main findings do not rely on isolated extreme values or marginal statistical significance, but on coherent and dynamically interpretable relationships. We have revised Section 2.3 to clarify these methodological considerations and improve transparency regarding data treatment prior to correlation analysis as following.

“The δ18O (δ18O is preferred because it is highly correlated with δD; r = 0.99), d-excess, and SA from the GV7-C ice core were used in the analysis. Two time periods (1957–2013 CE and 1872–2013 CE) were selected for correlation analyses between GV7-C records and climate datasets based on data availability (e.g., SAM indices) and to ensure adequate sample size. All datasets used in the correlation analyses were linearly detrended prior to computing correlations in order to emphasize interannual-to-decadal variability. Pearson correlation coefficients were calculated and their significance was assessed using a two-tailed Student’s t-test with corresponding p-values. Because both ice-core records and climate indices can exhibit serial autocorrelation (and smoothing further increases persistence), statistical significance should be interpreted conservatively. In addition, the large number of correlation tests (across variables, indices, seasons, and smoothing windows) can increase the chance of false positives; therefore, we emphasize correlation magnitude, temporal persistence, and physical consistency, and we interpret isolated significant correlations with caution. Smoothed time series (3- and 5-year running means) are used to highlight low-frequency coherence between variables. SAM and ENSO are considered key modes potentially affecting Antarctic climate variability (Turner et al., 2009; Cohen et al., 2012; Pohl et al., 2021; Wille et al., 2021), and the SOI and Niño3.4 indices describe Pacific variability that can influence the Southern Ocean and Antarctica (Meyerson et al., 2002; Bertler et al., 2004). ENSO teleconnections to Antarctica are transmitted through Rossby wave trains and associated circulation anomalies that are seasonally modulated, while the IOD is typically phase-locked to austral winter/spring conditions. SAM variability

influences Antarctic climate through shifts in the westerly wind belt and associated storm tracks. Because isotopic composition recorded in an annual layer reflects integrated snowfall through the year, GV7-C records represent the combined influence of seasonal processes. Climate data were therefore examined at both annual (January–December) and seasonal (DJF, MAM, JJA, SON) scales to assess potential relationships. Although some seasonal differences were observed, overall patterns and physical interpretations were consistent when annual means were used; therefore, annual values are presented to represent the net integrated climate signal preserved in the ice core.

For the 1957–2013 CE period, the following climate indices were compared with the annual means of the GV7-C ice core records: station-based SAM index (Marshall G and National Center for Atmospheric Research Staff, 2018), the Southern Oscillation Index (SOI) (https://www.ncei.noaa.gov/access/monitoring/enso/soi), Niño3.4 index (https://psl.noaa.gov/gcoswgsp/Timeseries/Nino34), Indian Ocean Dipole (IOD) index representing the SST gradient between the western and southeastern equatorial IO (https://psl.noaa.gov/gcos_wgsp/Timeseries/DMI), SST anomaly in the southeastern IO (SST-SEIO) (https://psl.noaa.gov/gcos_wgsp/Timeseries/DMI), and reconstructed sea ice extent (SIE) over the Ross–Amundsen Sea sector (162°E–250°E) and the East Antarctic sector (71°E–162°E) (Fogt et al., 2023). Moreover, for the 1957–2013 CE period, spatial correlation analysis (at 95% confidence interval) was conducted between annual GV7-C records and gridded ERA5 reanalysis data (air temperature, SST, sea ice concentration [SIC], 10-m wind speed, zonal [u] and meridional [v] wind components, and total precipitable water) using Climate Reanalyzer developed by the University of Maine, USA (https://climatereanalyzer.org/). Since ice-core isotopic signals reflect a broad range of thermodynamic and dynamic influences, spatial correlation analyses were conducted for physically plausible scenarios to help identify potential moisture supply regions over a longer time period (1957–2013 CE) than previous studies (Caiazzo et al., 2017; Khan, 2019). Spatially coherent and physically interpretable patterns are selectively presented and used as supportive evidence in the interpretation of climate-related signals from the GV7-C ice core. Principal component analysis (PCA), a linear dimensionality reduction technique, was employed to investigate potential similarities in variability between the annual means of the ice-core records and seasonal and annual means of climate datasets (IOD, SST-SEIO, SAM, SOI, Niño3.4, SIE) for 1957–2013 CE. The PCA results conducted on annual mean values were selected and presented in this study. For the 1872–2013 CE period, the GV7-C ice core data were compared with the IOD index, SST-SEIO, reconstructed SST anomaly over the Southern Hemisphere (https://www.ncei.noaa.gov/access/monitoring/climate-at-a-glance/global/time-

series) (Huang et al., 2017), reconstructed SAM index (https://psl.noaa.gov/data/20thC_Rean/timeseries/monthly/SAM), and Niño3.4."

- The results section presents correlation analyses between annual GV7-C records and annual/seasonal climate variables. Section 2.1 states that snow accumulation at the GV7-C site is higher during austral summer and autumn. This increased snow accumulation during these seasons will inevitably bias the GV7-C annual records ($\delta^{18}O$ and SA) and will consequently affect the results derived from correlating GV7-C annual records with ERA5 annual/seasonal climate variables. Failing to account for this seasonal bias in GV7-C records could lead to misleading interpretations of the relationship between these records and climate variables. Therefore, incorporating a seasonal bias assessment for GV7-C records and discussing this bias will improve the manuscript.

Answer: Thank you for the helpful comment, and we agree on the importance of considering seasonality of the ice core signals. In this study, the age of each sample depth was determined by interpolation between two consecutive $\delta^{18}O$ peaks, with an average of eight data points per year (ranging from 3 to 21). Consequently, some years did not contain sufficient data to represent all seasons or to construct reliable seasonal records for $\delta^{18}O$, d-excess, and SA. Therefore, annual values from the GV7-C record were used in this study.

- Section 2.2 indicates that "Annual layers were determined based on the seasonal summer maximum $\delta^{18}O$ peaks in the GV7-C ice core." While there is an explanation of how annual layers were identified, the manuscript lacks information on how the annual averages, which are used to generate most of the results, were calculated. Calculating annual averages from values between summer peaks will capture annual minima during austral winter but may disrupt the continuous representation of annual maxima during austral summer. This is particularly important because annual averages will reflect "better" the "continuous" season and introduce uncertainties regarding the representation of the "discontinuous" season. This approach can lead to some seasons being more prominently represented within the annual average, potentially skewing the correlations. Please provide additional information on how the annual averages were calculated and address the potential effects of divided seasons in both the results analysis and discussion.

Answer: Thank you for the comment regarding potential seasonal bias and the calculation of annual averages. The GV7-C age scale is based on consecutive summer δ18O maxima, and annual layers are defined accordingly. In the revised manuscript (Sect. 2.2), we now clarify that annual mean δ18O, δD, and d-excess values were computed as the arithmetic mean of all samples assigned to each annual layer (i.e.,

between two successive summer maxima). Because sampling density varies (3–21 samples per year; average 8), some years do not fully resolve all seasons; therefore, constructing continuous seasonal isotope series would introduce additional uncertainty. Annual means are therefore presented to represent the net integrated climatic imprint recorded in each annual layer, while acknowledging that annual signals are naturally weighted toward seasons with higher accumulation.

2.2 Ice core data

The 78 m long GV7-C ice core was collected over a total of 107 runs, and the average diameter of the ice core was measured to be an average diameter of 0.08 m. Density was estimated by measuring the mass and dimensions of the ice core subsections. The ice core sections were kept frozen and transported to Korea. Inside the cold room at the Korea Polar Research Institute (KOPRI), the ice core sections were cut to an average length of 0.04 m (ranged between 0.03 m and 0.07 m) for stable water isotopic analysis ($\delta^{18}O$ and δD). A total of 1880 samples were analyzed using cavity ring-down spectrometers (L2130-I and L2140-i, Picarro Inc., USA) at KOPRI. Annual layers were determined based on the seasonal summer maximum $\delta^{18}O$ peaks in the GV7-C ice core and the age of each sample depth was determined by interpolation between two consecutive peaks. The GV7-C ice core covers the period from 1782 to 2014 CE. The seasonal $\delta^{18}O$ pattern has been reported in previous studies (Caiazzo et al., 2017; Nardin et al., 2021). The annual layer counting of the ice core was confirmed and further constrained using the electrical conductivity measurement done by Portable ECM unit, Icefield Instruments Inc. Canada. The electrical conductivity peaks of Pinatubo (1991 CE), Agung (1963 CE), Tarawera (1886 CE), Krakatau (1883 CE), and Tambora (1815 CE) were used as additional time markers. The annual mean SA rate was calculated by multiplying the depth corresponding to one full year by the measured density of the ice core section, and was expressed in millimeters of water equivalent per year (mm w.e. yr^{-1}). The *d*-excess (*d*-excess = $\delta D - 8 \times \delta^{18}O$) was also calculated. Data points per year ranged from 3 to 21 (average 8), consequently, some years did not contain sufficient data to represent all seasons or to construct reliable seasonal records for $\delta^{18}O$, d-excess, and SA. Therefore, annual means of the GV7-C ice core records ($\delta^{18}O$, *d*-excess, and SA) were used in the correlation analysis presented in section 3.

- Section 3.2.1 lacks clarity in presenting the data. For instance, lines 188-190 do not explicitly state whether the authors are discussing the 10-m v wind or the 850 hPa v-wind. There also seems to be an inconsistency in reporting the positive or negative correlations between the Pacific Ocean (PO) and Indian Ocean (IO). Similarly, lines 193-194 mention positive correlations between annual d-excess and 2 m/850 hPa temperatures over the western PO and IO sectors. Figure S4 shows positive correlations between annual d-excess and 850 hPa temperatures over the IO sector, but there is no evidence supporting a positive correlation over the western PO sector. It would be very beneficial to include further information about the coverage of the PO and IO sectors, either in Figure 1 or within the text. Section 3.2.1 is complex and difficult to read, and the supporting plots do not provide complete information. For example, Figure S5 presents only the d-excess-SST spatial correlations for DJF and SON. Why are only these presented? Including the entire dataset (annual, DJF, MAM, JJA, and SON) would allow readers to understand how these spatial relationships change throughout the year. The same recommendation applies to all spatial correlations presented. Please reassess the clarity and organization of this section, as it is challenging to follow.

(from minor comment) Line 177: The correlations mentioned in this line cannot be directly traced to the figures in supporting evidence, making it difficult to evaluate the magnitude and spatial distribution of the correlations mentioned in the text. Please, provide figures for the correlations mentioned in the text or remove these statements from the text if the correlations are not relevant.

(from minor comment) Table 5: The table intends to summarise the observed correlations, however, it remains unclear the criteria that has to be met for a correlation to be included in the table and the table is not precise on the magnitude or sign of the correlation. Please, clarify.

Answer: Thank you for the comments related to the spatial correlation analysis and the clarity of Sect. 3.2. We revised the spatial-correlation discussion and reorganized the text into a dedicated Sect. 3.2.2 (Spatial correlation analysis with ERA5 reanalysis). The supplementary spatial-correlation results were consolidated and are now presented as three combined figures (Figs. S1–S3), focusing on the key, physically interpretable patterns that support our discussion. The revised text for Sect. 3.2.2 is provided below.

3.2.2. Spatial correlation analysis with ERA5 reanalysis

Spatial correlation analyses (95% confidence interval) were conducted between annual GV7-C records (δ18O, d-excess, and SA) and annual/seasonal ERA5 reanalysis fields for 1957–2013 CE to explore potential spatial patterns consistent with

moisture supply and transport pathways. Significant and physically interpretable patterns are selectively presented in the Supplement (Figs. S1–S3) and are used as supporting evidence in the discussion of likely source regions. For interpretation, the Pacific Ocean (PO) sector is defined here as the western Pacific (90–160°E), Ross Sea (160°E–130°W), and Amundsen–Bellingshausen Seas (130–60°W), while the Indian Ocean (IO) sector is defined as 20–90°E.

Annual mean δ18O shows positive correlations with 2 m air temperature and SST primarily over the PO sector (Fig. S1a, b). Positive relationships with air temperature (2 m and 850 hPa) and total column precipitable water are most evident during DJF over parts of the PO and IO sectors (Fig. S1d–f). Negative correlations are observed with sea ice concentration (SIC) over the Ross Sea region (Fig. S1c). Wind-speed correlations (10 m; annual and MAM) are generally negative (Fig. S1g, j), and zonal wind (u-wind) correlations highlight the belt of strong westerlies (Fig. S1h, k). The meridional wind (v-wind) correlations suggest a northward flow signature from the western PO sector and a southward flow signature from the IO sector during DJF (Fig. S1i), whereas these patterns weaken in MAM (Fig. S1l). Overall, δ18O exhibits its clearest spatial coherence during DJF and MAM, consistent with the seasonality of transport and snowfall in this coastal sector (Delmotte et al., 2000; Caiazzo et al., 2017). These patterns provide qualitative support for a relatively stronger PO-sector influence on δ18O at GV7-C during DJF–MAM, although the overall relationships remain modest.

Annual mean d-excess exhibits positive correlations with air temperature (2 m and 850 hPa) over both the western PO and IO sectors (Fig. S2a–c). Temperature correlations in the IO sector are particularly evident in SON (Fig. S2c), whereas the d-excess response to temperature appears weaker in DJF (not shown). Correlations with SST (SON), SIC (JJA), and total column precipitable water (annual) further support a contribution of air masses from the IO sector and western PO to the GV7 region (Fig. S2d–f). In contrast to δ18O, correlations with wind speed and wind direction are relatively weak, except for a positive correlation with 10 m wind speed in some regions (Fig. S2g). The v-wind pattern indicates a southward flow signature from the IO sector and a northward flow signature in the western PO sector (Fig. S2i). Taken together, these spatial patterns suggest that thermodynamic source-region variability (e.g., SST/air-temperature conditions) may play a comparatively larger role for d-excess at GV7-C than do purely dynamical indicators, and they are consistent with a potentially important contribution from the IO sector, particularly during SON.

No clear and temporally consistent relationships are observed between SA and the investigated climate variables; only weak and spatially limited patterns are identified (Fig. S3). For example, SA shows weak negative correlations with 2 m temperature over parts of the Amundsen Sea coast and weak positive correlations with total column precipitable water offshore of the Ross Sea coast (Fig. S3a, b). SA also shows

weak negative correlations with SIC over the Ross Sea region (Fig. S3c). Wind-speed correlations (10 m and 850 hPa) are weakly positive over parts of the PO sector (Fig. S3d, g), and the associated u- and v-wind patterns suggest modest transport signals (Fig. S3e, f, h, i). Overall, these results indicate that SA at GV7-C is likely influenced by multiple factors, including synoptic variability and transport efficiency, which may mask simple relationships with large-scale indices at annual resolution.

In sum, the spatial correlation patterns suggest that GV7-C records reflect regional variability linked to both the PO and IO sectors. The δ18O correlations that are most evident during DJF and MAM motivate consideration of SAM-related dynamical influences during these seasons, while d-excess more strongly reflects thermodynamic variability linked to the IO sector, particularly during SON (Masson-Delmotte et al., 2003).

Supplementary data

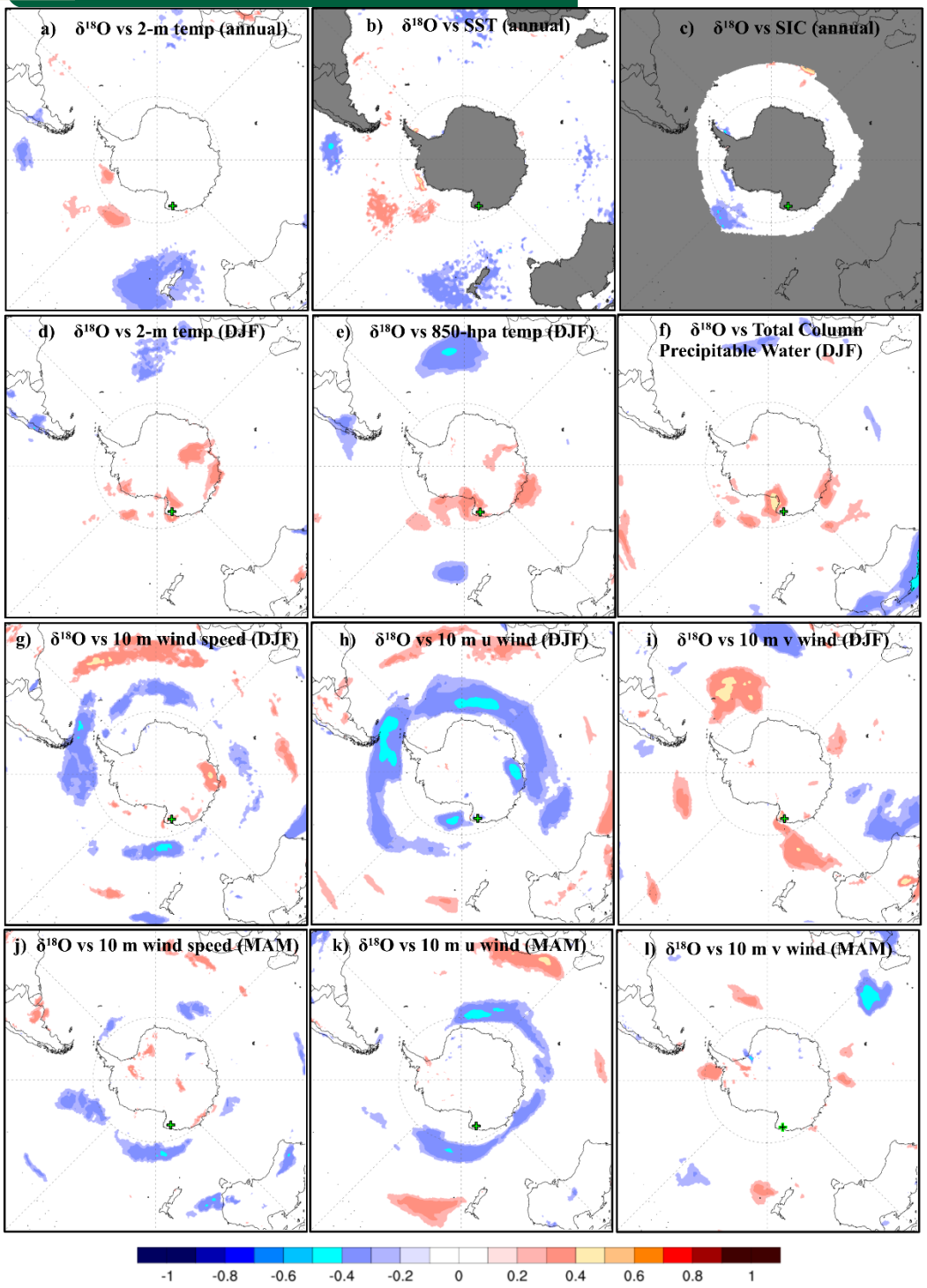

Figure S1. *Spatial correlation of $\delta^{18}O$ with (a, d, e) air temperature, (b) SST, and (c) SIC, (f) total column precipitable water, (g, j) wind speed, (h, k) u-wind components, and (i, l) v-wind components from the ERA5 reanalysis data for different seasons over the 1957–2013 CE period. The scale bars indicate Pearson's correlation coefficient (r) at $p < 0.05$. This figure was generated using Climate Reanalyzer (https://climatereanalyzer.org/) from the Climate Change Institute, University of Maine, USA.*

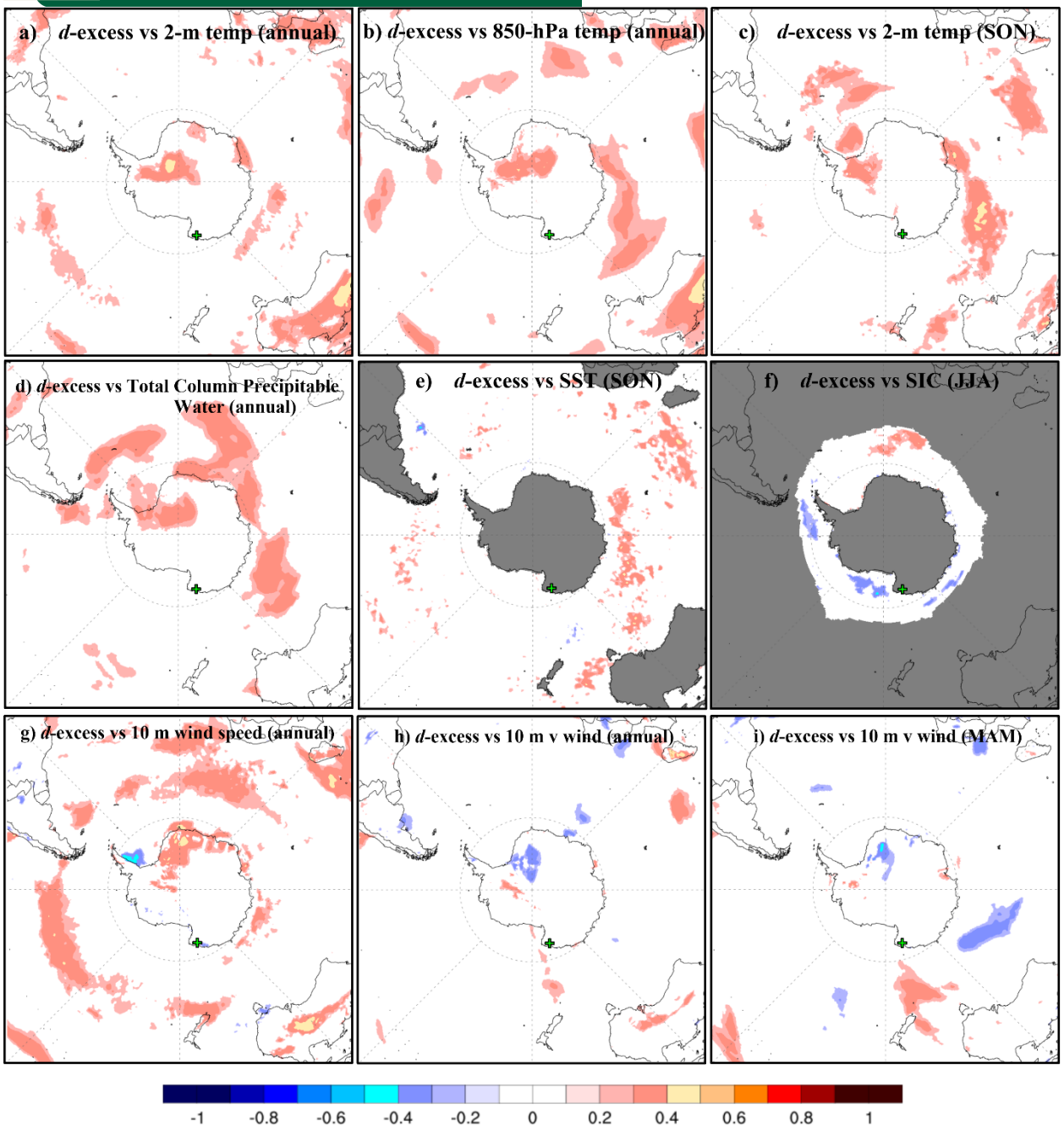

Figure S1. *Spatial correlation of d-excess with the (a, b, c) air temperature, (d) total column precipitable water, (e) SST, (f) SIC, (g) 10 m wind speed and (h, i) v-wind component from ERA5 reanalysis data for different seasons over the 1957–2013 CE period. The scale bars indicate Pearson's correlation coefficient (r) at $p < 0.05$. This figure was generated using Climate Reanalyzer (https://climatereanalyzer.org/) from the Climate Change Institute, University of Maine, USA.*

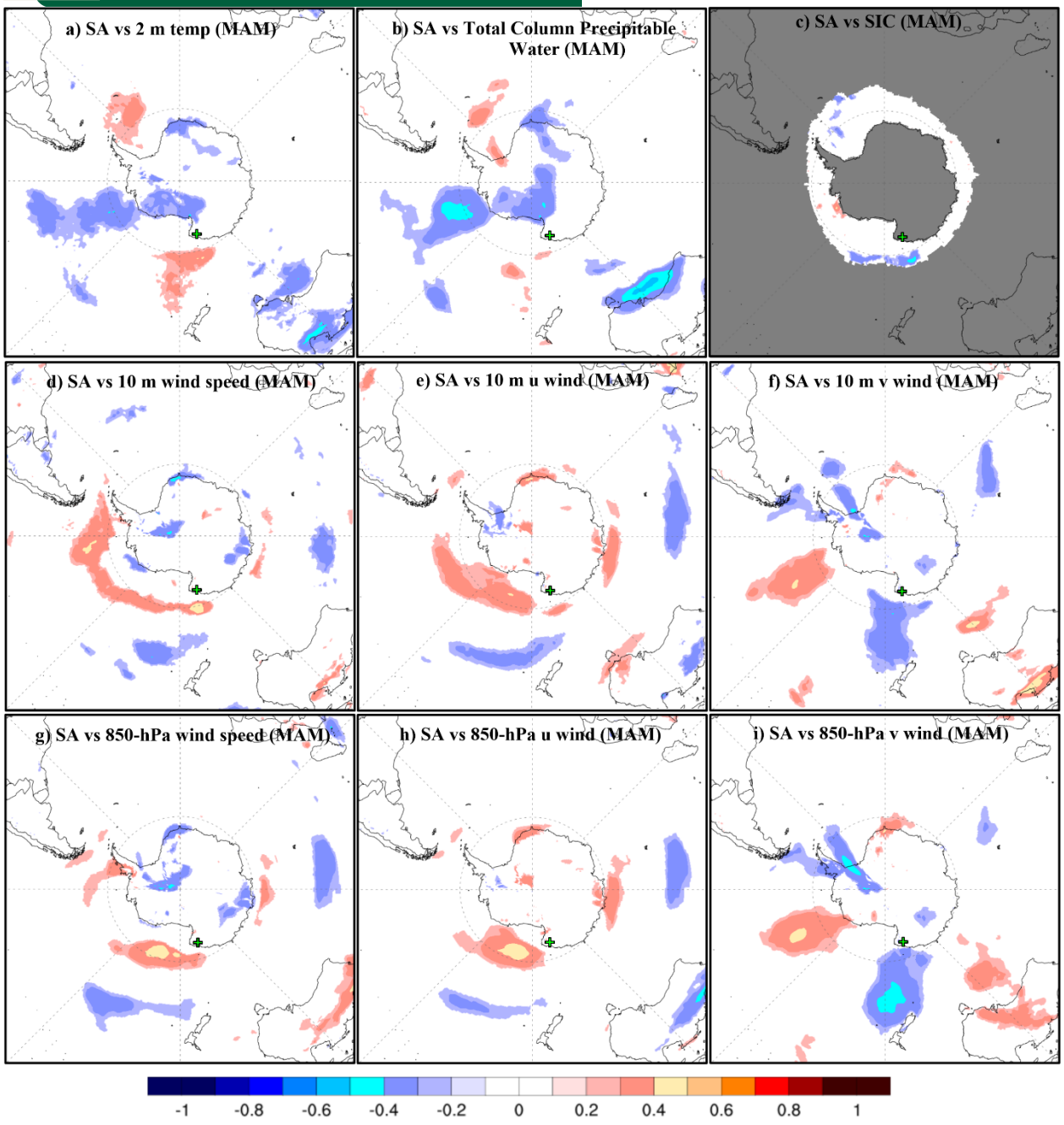

Figure S3. *Spatial correlation of SA with (a) air temperature, (b) total column precipitable water, (c) SIC, (d, g) 10 m wind speed, (e, h) u-wind components, and (f, i) v-wind components from ERA5 reanalysis data during the MAM season over the 1957–2013 CE period. The scale bars indicate Pearson's correlation coefficient (r) at $p < 0.05$. This figure was generated using Climate Reanalyzer (https://climatereanalyzer.org/) from the Climate Change Institute, University of Maine, USA.*

- Section 3.2.2 is quite challenging to read due to the amount of information presented without a clear structure. I recommend that the authors review the organization of this section, focusing on clearly conveying the main information relevant to supporting their arguments.

Answer: Thank you for the comment. We reorganized and streamlined this section to improve readability, removed duplications and unnecessary details, and clarified which spatial-correlation results are central to supporting our interpretations.

3.3 Climate Signals for the Long-Term Records (1872–2013 CE)

The GV7-C ice core data were also compared with long-term records (1872–2013 CE) for the SAM, Niño3.4, IOD, SST-SEIO, and SST anomaly over the Southern Hemisphere (Fig. 4 and Table 7). Pearson's correlation coefficients (r) are calculated for annual data and running averages. Three- and five-year averages were also calculated as comparison to the running averaged results, and the results were comparable (Table 7). For the $\delta^{18}O$ and SA, no significant correlations were found with the climate variables in the long-term analysis. This disappearance suggesting the smoothing of signal intensity due to various influencing factors. However, some evident relevance can still be observed in the short-term period for $\delta^{18}O$ and SA. The decrease in SA during the 1876–1885 CE and 1940–1955 CE periods was consistent with the increasing trend in the SAM, indicating the presence of cold and windy conditions during these periods. The recent trend (1985–2013) for $\delta^{18}O$ was also found to be in line with Niño3.4 and the SAM index (Fig. 4). Considering the correlation of $\delta^{18}O$ with Niño3.4 (r = 0.46) and SOI (r = –0.49) for 1957–2013 CE (Table 4), this suggests the influence of SST changes in the PO sector. However, this correlation weakened over a longer period (1872–2013).

While the *d*-excess was correlated with SST-SEIO (r = 0.43, n = 140, $p < 0.001$) and SST anomaly (r = 0.39, n = 148, $p < 0.001$) in the three-year averaged time series. Moreover, *d*-excess correlation was evident in the five-year running-averaged time series with the IOD (r = 0.30, n = 138, $p < 0.001$), SST-SEIO (r = 0.46, n = 138, $p < 0.001$), SAM (r = 0.3, n = 138, $p < 0.001$), and SST anomalies over the Southern Hemisphere (r = 0.43, n = 138, $p < 0.001$) (Table 7 and Fig. 4). The spatial correlation of *d*-excess with the reconstructed SST dataset was also tested for two periods: 1957–2013 CE, and 1854–2013 CE (Fig. 5). Weak positive correlations were observed over the remote IO sector during the 1957–2013 CE period (Fig. 5a) while in the period from 1854 to 2013 CE, the correlation was observed over a larger area in the southern sector of the IO (Fig. 5b). Consistently large peaks in the five-year running averaged time series for *d*-excess (both high and low values) were more frequent after 1845 (Fig. 4). Furthermore, it can be reported that the increasing phases in the global average temperature during the 1910–1945 CE period and since 1976 (IPCC, 2001) are evident in the increasing trend for *d*-excess (Fig. 4). The *d*-excess signal from the GV7-C ice core can be roughly suggested to representing thermodynamic changes (i.e., SST changes) over the IO sector of the Southern Ocean, at least over the 1872–2013 CE period.

Minor comments:

Line 25: Please consider specifying…large variations in the "near surface" air temperature….

Answer: Thank you for the helpful comment, we have edited accordingly.

1 Introduction

Climate variabilities over the Antarctica and the surrounding Southern Ocean is crucial for the global climate system (Mayewski et al., 2009; Fretwell et al., 2013; Rintoul et al., 2018). However, the Antarctic climate system is complex (Masson-Delmotte et al., 2008) relating to the large variations in the near surface air temperature (Nicolas and Bromwich, 2014; Constable et al., 2022) and surface mass balance (Dalaiden et al., 2020a), sparse observational data and its high variability

Line 39: Changes in atmospheric circulation "patterns"

Answer: Thank you for the helpful comment, we have edited accordingly.

1 Introduction

Climate variabilities over the Antarctica and the surrounding Southern Ocean is crucial for the global climate system (Mayewski et al., 2009; Fretwell et al., 2013; Rintoul et al., 2018). However, the Antarctic climate system is complex (Masson-Delmotte et al., 2008) relating to the large variations in the near surface air temperature (Nicolas and Bromwich, 2014; Constable et al., 2022) and surface mass balance (Dalaiden et al., 2020a), sparse observational data and its high variability (Kim et al., 2020; Klein et al., 2019). Particularly, the coastal regions of Antarctica show notable variations (Tuohy et al., 2015; Stenni et al., 2017; Goursaud et al., 2019). Using ice core records from Antarctica, the past climatic and environmental conditions can be reconstructed. The variations in the stable water isotopic compositions ($\delta^{18}O$ and δD) in ice cores are indicative of relative changes in the atmospheric temperature (Jouzel et al., 1997; Markle and Steig, 2022), sea ice extent (SIE), and atmospheric circulation (Thomas and Abram, 2016). Atmospheric circulation patterns have been reported as influential factors affecting the isotopic signals in ice cores (Bertler et al., 2004; Kino et al., 2021; Leroy-Dos Santos et al., 2023). The relationships between isotopes, temperature, and surface mass balance depend on the relative contributions of large-scale atmospheric dynamical and thermodynamic processes (Oerter et al., 2000; Medley et al., 2018; Goursaud et al., 2019; Dalaiden et al., 2020b).The effect of the Southern Annular Mode (SAM), which indicates the modulation of westerly winds towards the Southern Hemisphere (Hall and Visbeck, 2002; Fogt et al., 2012) were evidenced in the $\delta^{18}O$ and surface mass balance records

Lines 44-46: This sentence is not clear: "In recent decades, the Southern Annular Mode (SAM), which indicates the modulation of westerly winds towards the Southern Hemisphere (Hall and Visbeck, 2002; Fogt et al., 2012), has become increasingly important for the Southern Hemisphere climate (Russell and McGregor, 2010).". Does this mean that before the recent decades, SAM had no major relevance in the Southern Hemisphere climate? Please specify.

Answer: Thank you for the comment. We revised and reorganized the Introduction for clarity and to avoid wording that could imply that SAM was irrelevant prior to recent decades.

1 Introduction

Climate variabilities over the Antarctica and the surrounding Southern Ocean is crucial for the global climate system (Mayewski et al., 2009; Fretwell et al., 2013; Rintoul et al., 2018). However, the Antarctic climate system is complex (Masson-Delmotte et al., 2008) relating to the large variations in the near surface air temperature (Nicolas and Bromwich, 2014; Constable et al., 2022) and surface mass balance (Dalaiden et al., 2020a), sparse observational data and its high variability (Kim et al., 2020; Klein et al., 2019). Particularly, the coastal regions of Antarctica show notable variations (Tuohy et al., 2015; Stenni et al., 2017; Goursaud et al., 2019). Using ice core records from Antarctica, the past climatic and environmental conditions can be reconstructed. The variations in the stable water isotopic compositions ($\delta^{18}O$ and δD) in ice cores are indicative of relative changes in the atmospheric temperature (Jouzel et al., 1997; Markle and Steig, 2022), sea ice extent (SIE), and atmospheric circulation (Thomas and Abram, 2016). Atmospheric circulation patterns have been reported as influential factors affecting the isotopic signals in ice cores (Bertler et al., 2004; Kino et al., 2021; Leroy-Dos Santos et al., 2023). The relationships between isotopes, temperature, and surface mass balance depend on the relative contributions of large-scale atmospheric dynamical and thermodynamic processes (Oerter et al., 2000; Medley et al., 2018; Goursaud et al., 2019; Dalaiden et al., 2020b). The effect of the Southern Annular Mode (SAM), which indicates the modulation of westerly winds towards the Southern Hemisphere (Hall and Visbeck, 2002; Fogt et al., 2012) were evidenced in the $\delta^{18}O$ and surface mass balance records of coastal Antarctic ice cores (Schlosser et al., 2014; Servettaz et al., 2020). Moreover, the second-order parameter *d*-excess (*d*-excess = $\delta D - 8 \times \delta^{18}O$), which is sensitive to changes in the relative humidity and sea surface temperatures (SSTs) in the source region (Jouzel et al., 1982; Delmotte et al., 2000; Uemura et al., 2008), thus has been used to identify source regions (Stenni et al., 2001; Sodemann and Stohl., 2009). Furthermore, snow accumulation (SA) rates estimated from ice cores show a tendency to increase in warmer climates (Frieler et al., 2015; Palerme et al., 2017) and under low-sea ice conditions in coastal regions (Nyamgerel et al., 2020), being potential to reflect the surface air temperatures (Dalaiden et al., 2020a).
In recent decades, the SAM has become increasingly important for the Southern Hemisphere climate (Russell and McGregor, 2010), affecting the spatial variability of temperature, precipitation, and sea ice cover across Antarctica (Nicolas and Bromwich, 2014; Purich et al., 2016; Kim et al., 2020). The Antarctic surface mass balance is also linked with El Niño-Southern Oscillation (ENSO) (Kim et al., 2020). The teleconnection between the Antarctic and tropical climate have previously been reported in ice core records (Yuan, 2004; Schneider and Steig, 2008). However, this is still complex due to the instability over time and dependency on time scales under consideration and the concurrent state of the climate modes (e.g., ENSO and

Line 60: It is mentioned that the study aims to explore the climate-related signals in the GV7-C ice core record (including dD). However, the dD signal is not explored in depth (only included in the manuscript through the d-excess). Please include the dD record on the analyses or remove dD from the list of the records that will be explored in the study.

Answer: Thank you for the helpful comment, we mentioned about it in the following section.

2.3 Climate data and analysis

The $\delta^{18}O$ ($\delta^{18}O$ preferred and the correlation to δD is 0.99), *d*-excess, and SA from the GV7-C ice core were used in the analysis. Two time periods (1957–2013 CE and 1872–2013 CE) were considered in the correlation analysis between the GV7-C ice core and climate data. These periods were selected depending on the availability of the climate data (e.g., SAM index) and to ensure a large sample size. All data in the correlation analysis were detrended and the significance of the analysis assessed by a two-tailed student's t-test, and the significance of Pearson correlation coefficients was verified using the *p*-values. The SAM and ENSO are assumed to be factors that potentially affect the Antarctic climate (Turner et al., 2009; Cohen et al., 2012; Pohl et al., 2021; Wille et al., 2021) and the SOI and Niño3.4 indices describe changes in the PO that affect the climate over the Southern Ocean and Antarctic continent (Meyerson et al., 2002, Bertler et al., 2004). For this reason, for the 1957–2013 CE period, following climate indices were compared with the annual means of GV7-C ice core records; station-based SAM index (Marshall G and National Center for Atmospheric Research Staff, 2018), the Southern Oscillation Index

Line 72: it is mentioned that the site is 95km away from the coastline, however, the coastline is “permanently” covered with perennial sea ice (as seen in Fig 1). It would be useful to know how far is the site from the open water. Please add this info.

Answer: Thank you for the helpful comment. As you mentioned, depending on the perennial sea ice, the distance to open water (not the coastline) would be differed. We kept this mentioning the distance to coastline “of the Southern Ocean”, as it shown below.

2 Materials and methods

2.1 Study area

During the 2013/14 Antarctic summer season, a collaborative Italian/Korean expedition drilled several firn-ice cores at the GV7 drilling site (70°41′ S, 158°52′ E; 1950 m a.s.l.), located on the Oates Coast of East Antarctic (Fig. 1). Six shallow firn cores (ranging from 5 and 50 m in length) and intermediate firn-ice cores (ranging from 78 and 250 m in length) were drilled. The 78m deep core, named GV7-C, is used and presented in this study. The site is approximately 95 km away from the nearest coastline of the Southern Ocean, and the ice velocity at this location is very low (< 0.3 m yr^{-1}) (Frezzotti et al., 2007), and the 10-m firn temperature was measured to be –31.8 °C (Frezzotti et al., 2007). Notably, the SA rate in this area is relatively high,

Line 76-80: The information in these lines seem to disagree. The first line says that during autumn-winter airmasses primarily originate from WPO and during spring the from the Ross sector. Then, the next line says airmasses (2007-2012) are from the Indian Ocean and Antarctic Plateau with smaller contributions from the Ross Sea and PO. These sentences don’t say much unless the evaluation time period is specified in the first sentence. Please evaluate clarifying the information in these lines.

Answer: Thank you for the helpful comment, we have edited accordingly.

Frezzotti et al., 2007; Magand et al., 2004). Based on the records from 2007 to 2012, during the autumn–winter period, the air mass primarily originates from the western Pacific Ocean (PO) sector, while the spring period is characterized by dominant input from the Ross Sea sector, with prevailing winds from the south (Caiazzo et al., 2017). Back trajectory estimations revealed that the dominant air mass pathways are from the Indian Ocean (IO) (32%) and the Antarctic Plateau (29%) (Caiazzo et al., 2017), while the Ross Sea and western PO sectors account for 21% and 19%, respectively. Furthermore, the western PO

Line 82-83: Please specify which parameter is the one that exhibits the second maximum in winter. If it is the SA, please specify.

Answer: Thank you for the helpful comment, we have edited accordingly.

and IO sectors accounted for 59% (147 mm) and 28% (69 mm) of the total precipitation (250 mm), respectively (Caiazzo et al., 2017). The SA at this site was estimated to be higher in austral summer and autumn (Caiazzo et al., 2017). Notably, the western PO sector also exhibits a second maximum SA in winter, with the trajectory pathway indicating dominance from the Antarctica Plateau and the IO sector.

Figure1: Please add a reference to the geographical location of the oates coast. Figure 1: Please add elevation contours to the map. Figure 1: There are grey and green dots in the map, please add a legend stating what they mean

Answer: Thank you for your comment, we have edited accordingly. We excluded the lines representing the sea ice extent since it mentioned once only (not discussed further).

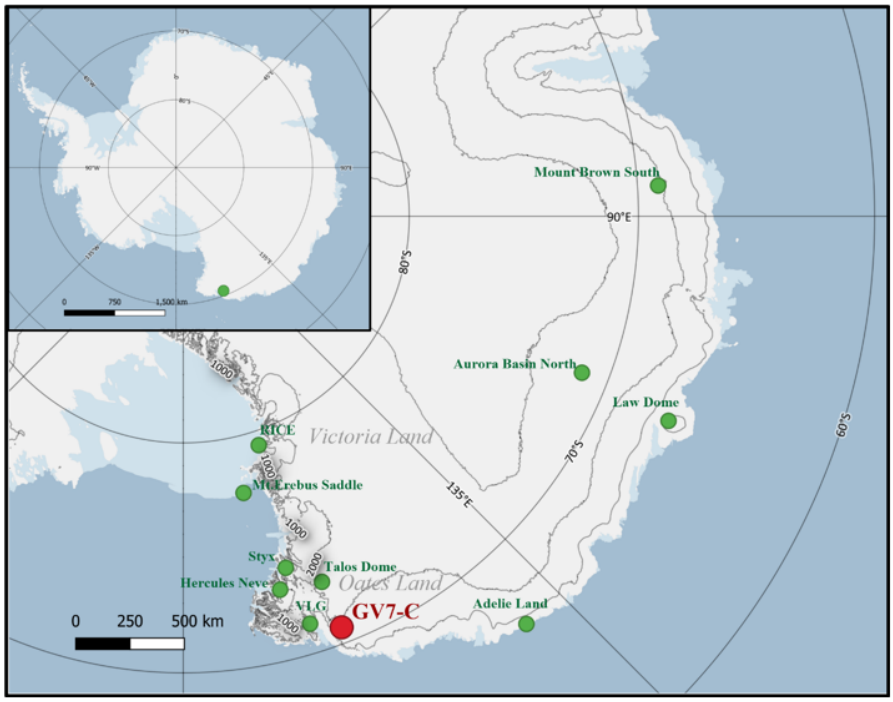

Figure 1. Location of the GV7-C ice core (red) and other ice core sites (green) in East Antarctica. RAMP2 elevation contours (1000 m) are shown (Liu et al., 2015). The map was generated using QGIS software with Quantarctica3 project data (Matsuoka et al., 2021).

Line 98: how was the electrical conductivity measured? Please, specify.

Answer: Thank you for the comment, we have edited accordingly.

2.1 Study area

During the 2013/14 Antarctic summer season, a collaborative Italian/Korean expedition drilled several firn-ice cores at the GV7 drilling site (70°41′ S, 158°52′ E; 1950 m a.s.l.), located on the Oates Coast of East Antarctic (Fig. 1). Six shallow firn cores (ranging from 5 and 50 m in length) and intermediate firn-ice cores (ranging from 78 and 250 m in length) were drilled. The 78m deep core, named GV7-C, is used and presented in this study. The site is approximately 95 km away from the nearest coastline of the Southern Ocean, and the ice velocity at this location is very low (< 0.3 m yr^{-1}) (Frezzotti et al., 2007), and the 10-m firn temperature was measured to be –31.8 °C (Frezzotti et al., 2007). Notably, the SA rate in this area is relatively high, while the post-depositional effect is low due to the low intensity of katabatic winds along the ice divide (Becagli et al., 2004;

Line 99-101: The manuscript doesn't mention about the SA estimation accounting for compression. Please specify why.

Answer: Thank you for the helpful comment, the annual mean SA rate was calculated in water-equivalent units by multiplying the depth corresponding to one full year by the measured density of each sections of the ice core. We also note that vertical strain thinning effect would be minimal given the shallow depth (78 m) and relatively short temporal coverage (233 years).

2.2 Ice core data

The 78 m long GV7-C ice core was collected over a total of 107 runs, and the average diameter of the ice core was measured to be an average diameter of 0.08 m. Density was estimated by measuring the mass and dimensions of the ice core subsections. The ice core sections were kept frozen and transported to Korea. Inside the cold room at the Korea Polar Research Institute (KOPRI), the ice core sections were cut to an average length of 0.04 m (ranged between 0.03 m and 0.07 m) for stable water isotopic analysis ($\delta^{18}O$ and δD). A total of 1880 samples were analyzed using cavity ring-down spectrometers (L2130-I and L2140-i, Picarro Inc., USA) at KOPRI. Annual layers were determined based on the seasonal summer maximum $\delta^{18}O$ peaks in the GV7-C ice core and the age of each sample depth was determined by interpolation between two consecutive peaks. The GV7-C ice core covers the period from 1782 to 2014 CE. The seasonal $\delta^{18}O$ pattern has been reported in previous studies (Caiazzo et al., 2017; Nardin et al., 2021). The annual layer counting of the ice core was confirmed and further constrained using the electrical conductivity measurement done by Portable ECM unit, Icefield Instruments Inc. Canada. The electrical conductivity peaks of Pinatubo (1991 CE), Agung (1963 CE), Tarawera (1886 CE), Krakatau (1883 CE), and Tambora (1815 CE) were used as additional time markers. The annual mean SA rate was calculated by multiplying the depth corresponding to one full year by the measured density of the ice core sections, and was expressed in millimeters of water equivalent per year (mm w.e. yr^{-1}). The *d*-excess (*d*-excess = $\delta D - 8 \times \delta^{18}O$) was also calculated. Data points per year ranged from 3 to 21 (average 8), consequently, some years did not contain sufficient data to represent all seasons or to construct reliable seasonal records for $\delta^{18}O$, d-excess, and SA. Therefore, annual means of the GV7-C ice core records ($\delta^{18}O$, *d*-excess, and SA) were used in the correlation analysis presented in section 3.

Lines 103-107: Please specify why the evaluation period goes back only to 1957, when ERA5 extends from 1950-present.

Answer: Thank you for the comment. We clarified in the Methods why two evaluation periods are used. The 1957–2013 CE period was selected to maximize overlap among the observational/reconstructed indices used (including SAM) and to ensure a robust and consistent comparison across datasets; the longer 1872–2013 CE period is used where longer climate reconstructions are available.

2.3 Climate data and analysis

The $\delta^{18}O$ ($\delta^{18}O$ preferred and the correlation with δD is 0.99), *d*-excess, and SA from the GV7-C ice core were used in the analysis. Two time periods (1957–2013 CE and 1872–2013 CE) were considered in the correlation analysis between the GV7-C ice core records and climate data. These periods were selected depending on the availability of the climate data (e.g., SAM index) and to ensure a large sample size. All datasets used in the correlation analysis were linearly detrended prior to analysis and the statistical significance of Pearson correlation coefficients was assessed using a two-tailed Student's *t* test

Line 127: The datasets are presented and evaluated in “periods”. Please specify in the methods section the reason to evaluate the datasets in these particular time periods.

Answer: Thank you for the helpful comment, we have edited the section 2.3. Climate data and analysis which was unclear about data processing. Two time periods (1957–2013 CE and 1872–2013 CE) were considered, plainly depending on the availability of the climate data (e.g., SAM index) and to ensure a large sample size compared to previous studies in this site. Now the edited parts can be seen as shown in below.

2.3 Climate data and analysis

The $\delta^{18}O$ ($\delta^{18}O$ preferred and the correlation with δD is 0.99), *d*-excess, and SA from the GV7-C ice core were used in the analysis. Two time periods (1957–2013 CE and 1872–2013 CE) were considered in the correlation analysis between the GV7-C ice core records and climate data. These periods were selected depending on the availability of the climate data (e.g., SAM index) and to ensure a large sample size. All datasets used in the correlation analysis were linearly detrended prior to analysis and the statistical significance of Pearson correlation coefficients was assessed using a two-tailed Student's *t*-test, and significance levels were verified using the corresponding *p*-values. Because climatic and ice-core time series may exhibit serial autocorrelation, which can reduce the effective degrees of freedom and potentially inflate nominal significance levels, statistical results are interpreted carefully. Emphasis is placed on correlation magnitude, temporal persistence, and physical consistency rather than solely on nominal *p*-values. Smoothed time series (3- and 5-year running means) were used to highlight low-frequency coherence between variables. The SAM and ENSO are assumed to be factors that potentially affect Antarctic climate variability (Turner et al., 2009; Cohen et al., 2012; Pohl et al., 2021; Wille et al., 2021), and the SOI and Niño3.4 indices describe changes in the Pacific Ocean that influence the Southern Ocean and Antarctic continent (Meyerson et al., 2002; Bertler et al., 2004). ENSO teleconnections to Antarctica are transmitted through Rossby wave trains and associated circulation anomalies, which are seasonally modulated, while the IOD is typically phase-locked to austral winter/spring conditions. Similarly, SAM variability influences Antarctic climate through shifts in the westerly wind belt and associated changes in storm tracks. Because the isotopic composition recorded in each annual ice-core layer represents the integrated snowfall accumulated throughout the year, the GV7-C record reflects the combined influence of seasonal processes. For this reason, climate data were initially examined at both annual (January to December) and seasonal (DJF, MAM, JJA, SON) scales to assess potential relationships with the GV7-C ice core data. Although some seasonal differences were observed, the overall patterns and physical interpretation remained consistent when annual means were used. Therefore, annual values were selected to represent the net integrated climate signal preserved in the ice core.

For the 1957–2013 CE period, the following climate indices were compared with the annual means of the GV7-C ice core records: station-based SAM index (Marshall G and National Center for Atmospheric Research Staff, 2018), the Southern Oscillation Index (SOI) (https://www.ncei.noaa.gov/access/monitoring/enso/soi), Niño3.4 index (https://psl.noaa.gov/gcoswgsp/Timeseries/Nino34), Indian Ocean Dipole (IOD) index representing the SST gradient between the western and southeastern equatorial IO (https://psl.noaa.gov/gcos_wgsp/Timeseries/DMI), SST anomaly in the southeastern IO (SST-SEIO) (https://psl.noaa.gov/gcos_wgsp/Timeseries/DMI), and reconstructed sea ice extent (SIE) over the Ross–Amundsen Sea sector (162°E–250°E) and the East Antarctic sector (71°E–162°E) (Fogt et al., 2023). Moreover, for the 1957–2013 CE period, spatial correlation analysis (at 95% confidence interval) was conducted between annual GV7-C records and gridded ERA5 reanalysis data (air temperature, SST, sea ice concentration [SIC], 10-m wind speed, zonal [u] and meridional [v] wind components, and total precipitable water) using Climate Reanalyzer developed by the University of Maine, USA (https://climatereanalyzer.org/). Since ice-core isotopic signals reflect a broad range of thermodynamic and dynamic influences, spatial correlation analyses were conducted for physically plausible scenarios to help identify potential moisture supply regions over a longer time period (1957–2013 CE) than previous studies (Caiazzo et al., 2017; Khan, 2019). Only spatially coherent and physically interpretable patterns are selectively presented and used as supportive evidence in the interpretation of climate-related signals from the GV7-C ice core. Principal component analysis (PCA), a linear dimensionality reduction technique, was employed to investigate potential similarities in variability between the annual means of the ice-core records and seasonal and annual means of climate datasets (IOD, SST-SEIO, SAM, SOI, Niño3.4, SIE) for 1957–2013 CE. The PCA results conducted on annual mean values were selected and presented in this study. For the 1872–2013 CE period, the GV7-C ice core data were compared with the IOD index, SST-SEIO, reconstructed SST anomaly over the Southern Hemisphere (https://www.ncei.noaa.gov/access/monitoring/climate-at-a-glance/global/time-series) (Huang et al., 2017), reconstructed SAM index (https://psl.noaa.gov/data/20thC_Rean/timeseries/monthly/SAM), and Niño3.4.

Line 129: It is mentioned six periods, however, Figure 2 shows seven periods and there are seven periods in between brackets in line 130. Please, correct for consistency.

Answer: Thank you for the comment, we have edited accordingly.

3.1 Characterization of the GV7-C ice core record

The descriptive statistics for the annual mean $\delta^{18}O$, δD, *d*-excess, and SA in the GV7-C ice core are presented in Table 1. The results are also presented in five different time scales at around 50-year intervals (Table 1). For the whole 1782–2013 CE period, the annual mean $\delta^{18}O$ in the GV7-C ice core (n = 233) fluctuated between –32.92‰ and –24.60‰, while δD ranged from –259.42‰ to –210.21‰. The annual variation in $\delta^{18}O$, *d*-excess, and SA is presented in Figure 2, revealing large interannual and decadal-scale variations. Sequential years (at least five) with smaller (or colder) than average $\delta^{18}O$ (–29.64‰) were observed for seven periods (1838–1842 CE, 1858–1862 CE, 1880–1885 CE, 1904–1908 CE, 1918–1922 CE, 1960–1965 CE, and 1995–2002 CE). Additionally, the years between 1977 and 1991 were lower than average, except for 1979, 1982,

Line 132: Is mentioned that there are four periods with sequential years higher than the average. However, figure 2 only shows three periods. Please, correct for consistency.

Answer: Thank you for the comment, we have edited accordingly.

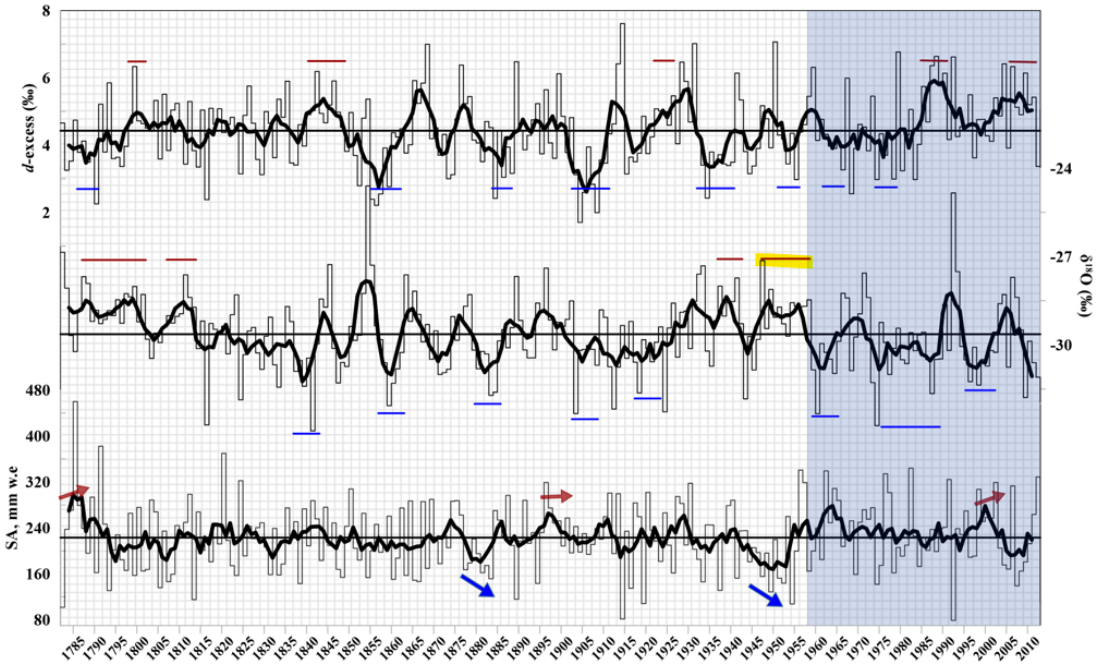

Figure 2. Temporal variation in the SA (bottom panel), $\delta^{18}O$ (middle panel), and *d*-excess (top panel), with the horizontal black line indicating the overall mean. The thick black lines represent the 5-year running average. The blue and red lines (arrows) indicate the periods that are higher or lower than average for at least four continuous years.

Line 132: Periods are reported without a temporal unit (CE), not matching previously reported periods in Line 130.

Answer: Thank you, we have edited accordingly.

3.1 Characterization of the GV7-C ice core record

The descriptive statistics for the annual mean $\delta^{18}O$, δD, *d*-excess, and SA in the GV7-C ice core are presented in Table 1. The results are also presented in five different time scales at around 50-year intervals (Table 1). For the whole 1782–2013 CE period, the annual mean $\delta^{18}O$ in the GV7-C ice core (n = 233) fluctuated between −32.92‰ and −24.60‰, while δD ranged from −259.42‰ to −210.21‰. The annual variation in $\delta^{18}O$, *d*-excess, and SA is presented in Figure 2, revealing large interannual and decadal-scale variations. Sequential years (at least five) with smaller (or colder) than average $\delta^{18}O$ (−29.64‰) were observed for seven periods (1838–1842 CE, 1858–1862 CE, 1880–1885 CE, 1904–1908 CE, 1918–1922 CE, 1960–1965 CE, and 1995–2002 CE). Additionally, the years between 1977 CE and 1991 CE were lower than average, except for 1979 CE, 1982 CE, 1985 CE, and 1990 CE. In addition, sequential years (at least six) higher than the average were observed for 1787–1801 CE, 1807–1813 CE, 1937–1942 CE, and 1948–1958 CE (except 1953) (Fig. 2). The linear relationship between $\delta^{18}O$ and δD ($\delta D = 8.46 \times \delta^{18}O + 17.97$, $R^2 = 0.99$, n = 1880, $p < 0.001$) had a slope slightly larger than that for the precipitation isotopic composition both globally (8) (Craig, 1961) and on the Antarctic–wide scale (7.75) (Masson-Delmotte et al., 2008). The slopes derived for the different time scales ranged from 8.35 (for 1982–2013 CE) to 8.67 (for 1882–1931 CE) (Table 2).

Line 138-139: The manuscript lists eight periods while Figure 2 only highlights seven. Please, correct for consistency.

Answer: Thank you for the helpful comment, we have edited accordingly.

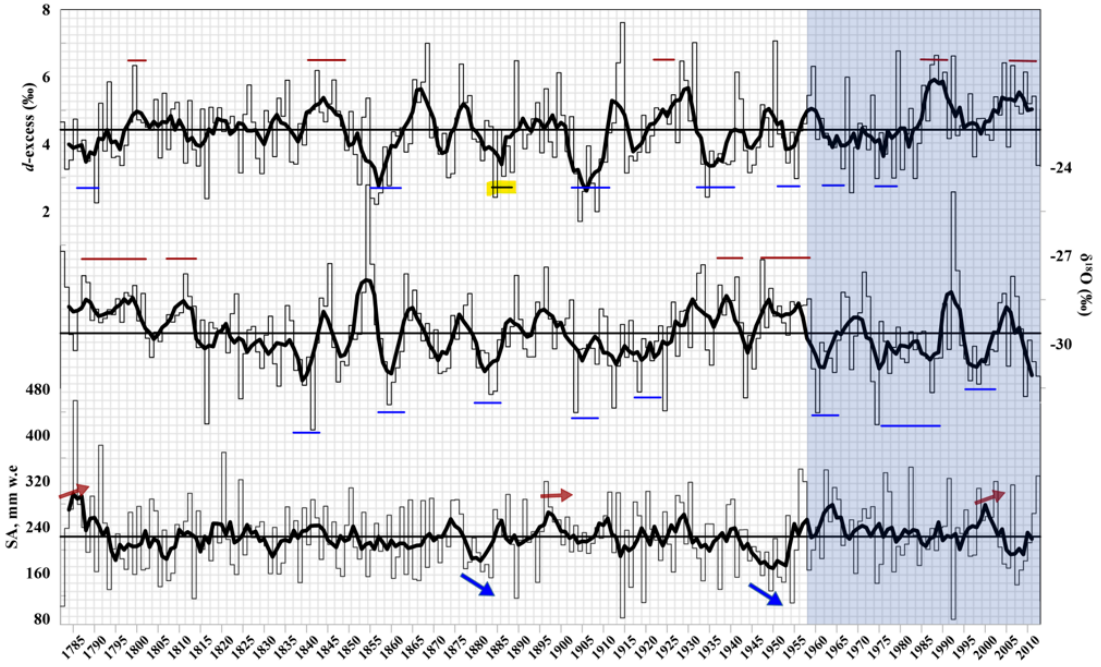

Figure 2. Temporal variation in the SA (bottom panel), $\delta^{18}O$ (middle panel), and *d*-excess (top panel), with the horizontal black line indicating the overall mean. The thick black lines represent the 5-year running average. The blue and red lines (arrows) indicate the periods that are higher or lower than average for at least four continuous years.

Table 1,2 & 3: The evaluation periods have higher "n" values than the annual evaluation. Please specify in the methods section what data is being used when comparing the evaluation "periods"

Answer: Thank you for the helpful comment, we have edited accordingly. Table 2 and 3 are combined in one table and we reorganized as it shown in below. We also mentioned it in 3.1. section.

Table 2. Linear regression analysis for $\delta^{18}O$ with δD and *d*-excess from the GV7-C ice core.

	Slope	Intercept	R^2	*p*-value	n
		$\delta^{18}O$ vs δD			
1782–2013 CE (all data)	8.46	17.97	0.99	<0.0001	1880
1782–1831 CE	8.54	20.12	0.99	<0.0001	344
1832–1881 CE	8.44	17.60	0.99	<0.0001	355
1882–1931 CE	8.67	24.36	0.99	<0.0001	399
1932–1981 CE	8.51	19.41	0.99	<0.0001	429
1982–2013 CE	8.35	15.51	0.99	<0.0001	353
Annual mean	8.17	9.64	0.99	<0.0001	233
Annual maximum	8.27	13.57	0.98	<0.0001	233
Annual minimum	8.19	9.07	0.99	<0.0001	233
		$\delta^{18}O$ vs *d*-excess			
1782–2013 CE (all data)	0.46	18.07	0.21	<0.0001	1880
1782–1831 CE	0.54	20.04	0.24	<0.0001	344
1832–1881 CE	0.45	17.83	0.18	<0.0001	355
1882–1931 CE	0.67	24.33	0.34	<0.0001	399
1932–1981 CE	0.52	19.45	0.24	<0.0001	429
1982–2013 CE	0.36	15.62	0.18	<0.0001	353
Annual mean	0.18	9.68	0.04	<0.0001	233
Annual maximum	0.28	14.45	0.10	<0.0001	233
Annual minimum	0.26	10.68	0.09	<0.0001	233

3 Results and discussion

3.1 Characterization of the GV7-C ice core record

The descriptive statistics for the annual mean $\delta^{18}O$, δD, *d*-excess, and SA in the GV7-C ice core are presented in Table 1. The results are also presented in five different time scales at around 50-year intervals (Table 1). Linear regression of $\delta^{18}O$ with δD and *d*-excess were reported for all data and the five different time scales, as well as for annually averaged values, annual maxima, and annual minima (Table 3). For the whole 1782–2013 CE period, the annual mean $\delta^{18}O$ in the GV7-C ice core (n = 233) fluctuated between –32.92‰ and –24.60‰, while δD ranged from –259.42‰ to –210.21‰. The annual variation in

Line 178-179: the manuscript brings attention to “the correlations”, however, it remains unclear to which correlations the authors are referring (positive? negative?). Please, clarify.

Answer: Thank you for the comment, we have edited accordingly.

“The annual mean of $\delta^{18}O$ had positive correlations with the air temperature, SST, total precipitable water, and GPH changes, while negative correlations were observed with the SIC and wind speed (Figs. S1–S3). These correlations with $\delta^{18}O$ were predominantly observed during the austral summer (DJF) and autumn (MAM) seasons (Table 6). Figure 3: Please add values to each vertical axis for reference.”

We used the standardized profiles of the variable in Figure 3 without y-axis values just for better visualization (avoiding too many visual objects) for comparing the variations of these multiple lines (if necessary, we are able to add). We edited coloring of the ice core records and y-axis titles as well, and added SST-SEIO line which was absent the previous version to align with the variables discussed in the correlation analysis for 1957–2013 CE period.

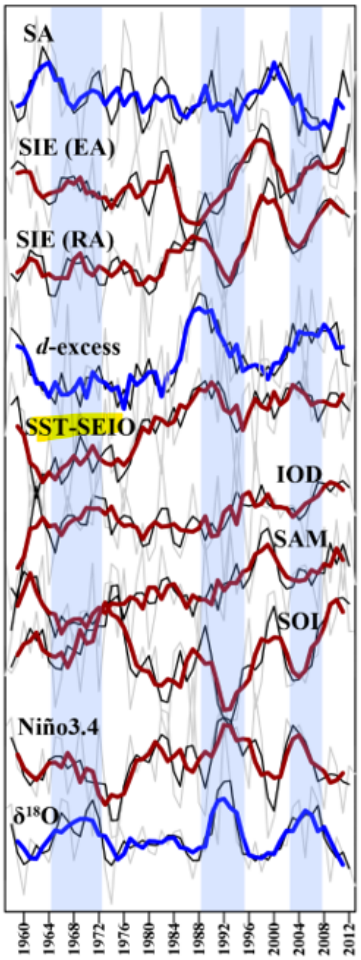

Figure 3. Comparison of the standardized profiles (grey lines) for SA, $\delta^{18}O$, and *d*-excess with the climate variables for 1957–2013 CE. The thin black and thick lines (blue and red) indicate the 3- and 5-year running average. The vertical red shading indicates periods with large $\delta^{18}O$ values.

Line 297: the manuscript states correlations were performed using the running-averaged data. Why not the non-averaged data? Also, it seems that they only used the 5-year running-averaged data. Why not the 3-year running-averaged data? It is not clear from the manuscript why they use some datasets and not all the ones they generated.

Answer: Thank you for the helpful comment, again helped us to reconsider the concise reporting of the results. We have added results for annual averages for 1957–2013 and 1872–2013, and edited the table captions (which was unclear in the previous version).

Table 4. Pearson's correlation coefficients (r) between the GV7-C ice core records and the climate variables for the period 1957–2013 CE. Correlations are calculated for annual data, running averages, and three- and five-year averages (shown in parentheses). Larger values ($r > 0.3$ at $p < 0.05$) are marked in underlined bold. SIE (EA) and SIE (RA) denotes sea ice extent over East Antarctica and the Ross-Amundsen Sea sector.

	IOD	SST (SEIO)	SAM	SOI	Niño3.4	SIE (EA)	SIE (RA)
				Annual average			
SA	0.28	–0.26	0.04	–0.01	0.04	–0.02	0.00
$\delta^{18}O$	–0.03	–0.07	–0.18	–0.26	0.22	–0.07	–0.22
d-excess	–0.07	**0.33**	0.09	0.03	0.05	0.02	0.22
				3-yr running average (three-year average)			
SA	0.18 (0.10)	**–0.36 (–0.52)**	–0.06 (–0.13)	0.09 (–0.04)	–0.14 (0.07)	0.04 (0.19)	–0.02 (–0.22)
$\delta^{18}O$	–0.02 (–0.27)	0.04 (0.14)	–0.27 **(–0.43)**	**–0.49 (–0.54)**	**0.46 (0.49)**	–0.11 (–0.27)	**–0.32 (–0.33)**
d-excess	–0.06 (–0.17)	**0.72 (0.81)**	0.21 (0.08)	–0.09 (–0.16)	0.27 (0.37)	–0.16 (–0.21)	0.31 (0.30)
				5-yr running average (five-year average)			
SA	–0.10 (–0.06)	**–0.42 (–0.40)**	–0.11 (–0.22)	0.10 (–0.08)	–0.20 (–0.01)	–0.03 (–0.28)	–0.15 (–0.16)
$\delta^{18}O$	0.00 (–0.22)	0.11 (–0.13)	–0.25 **(–0.41)**	**–0.44 (–0.42)**	**0.49 (0.39)**	–0.15 **(–0.41)**	–0.27 (–0.29)
d-excess	0.08 (0.01)	**0.79 (0.70)**	**0.37** (0.10)	–0.13 (–0.25)	**0.32 (0.52)**	–0.12 (–0.22)	**0.47** (0.27)

Table 7. Pearson's correlation coefficients (r) between the GV7-C ice core records and the climate variables for the period 1872–2013 CE. Correlations are calculated for annual data, running averages, and three- and five-year averages (shown in parentheses). Larger values ($r > 0.3$ at $p < 0.05$) are marked in underlined bold.

	IOD	SST (SEIO)	SST anomaly	SAM	Niño3.4
			Annual		
SA	0.10	–0.11	–0.01	0.03	0.02
$\delta^{18}O$	–0.04	–0.02	–0.08	–0.14	0.13
d-excess	–0.04	–0.02	–0.08	–0.14	0.13
			3-yr running average (three-year average)		
SA	0.01 (–0.07)	0.02 (–0.01)	0.02 (–0.06)	0.09 (–0.02)	0.03 (0.07)
$\delta^{18}O$	–0.11 (–0.16)	–0.02 (–0.17)	–0.11 (–0.20)	–0.16 (–0.19)	0.18 (0.18)
d-excess	0.23 (0.29)	**0.43 (0.41)**	**0.39 (0.40)**	0.24 (0.25)	0.26 (0.35)
			5-yr running average (five-year average)		
SA	–0.04 (–0.09)	0.11 (0.16)	0.04 (0.14)	0.07 (0.18)	0.15 (–0.03)
$\delta^{18}O$	–0.09 (–0.05)	–0.03 (–0.05)	–0.11 (–0.03)	–0.14 (–0.05)	0.12 (0.07)
d-excess	**0.30 (0.73)**	**0.46 (0.78)**	**0.43 (0.76)**	**0.30 (0.71)**	0.16 (0.36)

We also edited the result section which quite wordy and unclear.

3.2 Climate signals for the 1957–2013 CE period

3.2.1. Correlation with large-scale climate modes

The SAM, Niño3.4, SOI, as well as IOD, and SIE data were compared with the $\delta^{18}O$, *d*-excess, SA of the GV7-C ice core. The standardized values of the variables for 1957–2013 CE are presented in Figure 3. The $\delta^{18}O$ exhibited three periods of higher values (1964–1971 CE, 1989–1993 CE, and 2001–2007 CE) (Fig. 3), while the *d*-excess remained generally flat before 1983 and showed two periods of higher values (1985–1992, 2002–2011). The SA values showed significant interannual variations. Pearson's correlation coefficients (r) between the GV7-C ice core records and the climate variables are shown in Table 4. Correlations are calculated for annual data and running averages. Three- and five-year averages were also calculated as comparison to the running averaged results, and the results were comparable (Table 4). For the annual mean time series, no significant correlations were found, except that *d*-excess show a weak correlation to SST-SEIO ($r = 0.33, p < 0.05, n = 57$). Furthermore, *d*-excess had moderate positive correlation with SST-SEIO ($r = 0.72$, $p < 0.001$ $n = 54$) in the three-year running-averaged time series. In the five-year smoothed time series, *d*-excess kept the correlation with SST-SEIO ($r = 0.79$, $p < 0.001$ $n = 53$), and showed a weak positive correlation with the SAM ($r = 0.37$, $p < 0.005$, $n = 52$), Niño3.4 ($r = 0.32$, $p < 0.05$, $n = 52$), and SIE over the Ross-Amundsen Sea ($r = 0.47$, $p < 0.001$, $n = 52$). While the $\delta^{18}O$ exhibited correlations with Niño3.4 ($r = 0.46$, $p < 0.001$, $n = 54$), SOI ($r = -0.49$, $p < 0.001$, $n = 54$), and SIE over the Ross-Amundsen Sea ($r = -0.32$, $p < 0.05$, $n = 55$) in the five-year running-averaged time series. The correlations with Niño3.4 and SOI were persistent in the five-year running-averaged time series. For SA, weak negative correlation was observed only with SST-SEIO in the three- and five-year running-averaged time series, which is difficult to explain by increased evaporation under warmer conditions. Overall, the correlation analysis likely to suggest the variations in the *d*-excess (for the 1957–2013 CE) capture the climatic signals (sea surface temperature) over the southeastern IO, and this relevance indicate the air mass intrusion from this region. While the $\delta^{18}O$ likely to indicates the detectability of climatic signals over the tropical PO as well as the southern sector of the PO, indicating the contribution of air mass originating from this region.

3.3 Climate Signals for the Long-Term Records (1872–2013 CE)

The GV7-C ice core data were also compared with long-term records (1872–2013 CE) for the SAM, Niño3.4, IOD, SST-SEIO, and SST anomaly over the Southern Hemisphere (Fig. 4 and Table 7). Pearson's correlation coefficients (r) are calculated for annual data and running averages. Three- and five-year averages were also calculated as comparison to the running averaged results, and the results were comparable (Table 7). For the $\delta^{18}O$ and SA, no significant correlations were found with the climate variables in the long-term analysis. This disappearance suggesting the smoothing of signal intensity due to various influencing factors. However, some evident relevance can still be observed in the short-term period for $\delta^{18}O$ and SA. The decrease in SA during the 1876–1885 CE and 1940–1955 CE periods was consistent with the increasing trend in the SAM, indicating the presence of cold and windy conditions during these periods. The recent trend (1985–2013) for $\delta^{18}O$ was also found to be in line with Niño3.4 and the SAM index (Fig. 4). Considering the correlation of $\delta^{18}O$ with Niño3.4 ($r = 0.46$) and SOI ($r = -0.49$) for 1957–2013 CE (Table 4), this suggests the influence of SST changes in the PO sector. However, this correlation weakened over a longer period (1872–2013).

While the *d*-excess was correlated with SST-SEIO ($r = 0.43$, $n = 140$, $p < 0.001$) and SST anomaly ($r = 0.39$, $n = 148$, $p < 0.001$) in the three-year averaged time series. Moreover, *d*-excess correlation was evident in the five-year running-averaged time series with the IOD ($r = 0.30$, $n = 138$, $p < 0.001$), SST-SEIO ($r = 0.46$, $n = 138$, $p < 0.001$), SAM ($r = 0.3$, $n = 138$, $p < 0.001$), and SST anomalies over the Southern Hemisphere ($r = 0.43$, $n = 138$, $p < 0.001$) (Table 7 and Fig. 4). The spatial correlation of *d*-excess with the reconstructed SST dataset was also tested for two periods: 1957–2013 CE, and 1854–2013 CE (Fig. 5). Weak positive correlations were observed over the remote IO sector during the 1957–2013 CE period (Fig. 5a) while in the period from 1854 to 2013 CE, the correlation was observed over a larger area in the southern sector of the IO (Fig. 5b). Consistently large peaks in the five-year running averaged time series for *d*-excess (both high and low values) were more frequent after 1845 (Fig. 4). Furthermore, it can be reported that the increasing phases in the global average temperature during the 1910–1945 CE period and since 1976 (IPCC, 2001) are evident in the increasing trend for *d*-excess (Fig. 4). The *d*-excess signal from the GV7-C ice core can be roughly suggested to representing thermodynamic changes (i.e., SST changes) over the IO sector of the Southern Ocean, at least over the 1872–2013 CE period.

Lines 312-324: it is not clear if the authors are reporting results obtained using the 3-year or 5-year running-averaged data. Please specify.

Answer: Thank you for the comment. We revised the Results section to explicitly state when 3-year versus 5-year running means are used and to make the presentation of smoothed versus unsmoothed results clearer.

3.3 Climate Signals for the Long-Term Records (1872–2013 CE)

The GV7-C ice core data were also compared with long-term records (1872–2013 CE) for the SAM, Niño3.4, IOD, SST-SEIO, and SST anomaly over the Southern Hemisphere (Fig. 4 and Table 7). Pearson's correlation coefficients (r) are calculated for annual data and running averages. Three- and five-year averages were also calculated as comparison to the running averaged results, and the results were comparable (Table 7). For the $\delta^{18}O$ and SA, no significant correlations were found with the climate variables in the long-term analysis. This disappearance suggesting the smoothing of signal intensity due to various influencing factors. However, some evident relevance can still be observed in the short-term period for $\delta^{18}O$ and SA. The decrease in SA during the 1876–1885 CE and 1940–1955 CE periods was consistent with the increasing trend in the SAM, indicating the presence of cold and windy conditions during these periods. The recent trend (1985–2013) for $\delta^{18}O$ was also found to be in line with Niño3.4 and the SAM index (Fig. 4). Considering the correlation of $\delta^{18}O$ with Niño3.4 (r = 0.46) and SOI (r = –0.49) for 1957–2013 CE (Table 4), this suggests the influence of SST changes in the PO sector. However, this correlation weakened over a longer period (1872–2013).

While the *d*-excess was correlated with SST-SEIO (r = 0.43, n = 140, $p < 0.001$) and SST anomaly (r = 0.39, n = 148, $p < 0.001$) in the three-year averaged time series. Moreover, *d*-excess correlation was evident in the five-year running-averaged time series with the IOD (r = 0.30, n = 138, $p < 0.001$), SST-SEIO (r = 0.46, n = 138, $p < 0.001$), SAM (r = 0.3, n = 138, $p < 0.001$), and SST anomalies over the Southern Hemisphere (r = 0.43, n = 138, $p < 0.001$) (Table 7 and Fig. 4). The spatial correlation of *d*-excess with the reconstructed SST dataset was also tested for two periods: 1957–2013 CE, and 1854–2013 CE (Fig. 5). Weak positive correlations were observed over the remote IO sector during the 1957–2013 CE period (Fig. 5a) while in the period from 1854 to 2013 CE, the correlation was observed over a larger area in the southern sector of the IO (Fig. 5b). Consistently large peaks in the five-year running averaged time series for *d*-excess (both high and low values) were more frequent after 1845 (Fig. 4). Furthermore, it can be reported that the increasing phases in the global average temperature during the 1910–1945 CE period and since 1976 (IPCC, 2001) are evident in the increasing trend for *d*-excess (Fig. 4). The *d*-excess signal from the GV7-C ice core can be roughly suggested to representing thermodynamic changes (i.e., SST changes) over the IO sector of the Southern Ocean, at least over the 1872–2013 CE period.

Table 8: I find very difficult to understand this table. What does the number inside the parenthesis mean? The caption says "Pearson's correlation coeficcients between three- and five-year average (in parenthesis) and…". According to what is written in the caption, I understand that what it is in parenthesis is the five-year average correlation coefficient. However, the last four rows of the table are exclusively dedicated to presenting the data for the 5-year running-average dataset and it also has numbers in parenthesis. Please consider adding information in the table caption about how to interpret table 8.

Answer: Thank you for the helpful comment, we have edited the table captions (which was unclear in the previous version).

Table 4. Pearson's correlation coefficients (r) between the GV7-C ice core records and the climate variables for the period 1957–2013 CE. Correlations are calculated for annual data, running averages, and three- and five-year averages (shown in parentheses). Larger values ($r > 0.3$ at $p < 0.05$) are marked in underlined bold. SIE (EA) and SIE (RA) denotes sea ice extent over East Antarctica and the Ross-Amundsen Sea sector.

	IOD	SST (SEIO)	SAM	SOI	Niño3.4	SIE (EA)	SIE (RA)
				Annual average			
SA	0.28	–0.26	0.04	–0.01	0.04	–0.02	0.00
$\delta^{18}O$	–0.03	–0.07	–0.18	–0.26	0.22	–0.07	–0.22
d-excess	–0.07	**0.33**	0.09	0.03	0.05	0.02	0.22
				3-yr running average (three-year average)			
SA	0.18 (0.10)	**–0.36 (–0.52)**	–0.06 (–0.13)	0.09 (–0.04)	–0.14 (0.07)	0.04 (0.19)	–0.02 (–0.22)
$\delta^{18}O$	–0.02 (–0.27)	0.04 (0.14)	–0.27 **(–0.43)**	**–0.49 (–0.54)**	**0.46 (0.49)**	–0.11 (–0.27)	**–0.32 (–0.33)**
d-excess	–0.06 (–0.17)	**0.72 (0.81)**	0.21 (0.08)	–0.09 (–0.16)	0.27 (0.37)	–0.16 (–0.21)	0.31 (0.30)
				5-yr running average (five-year average)			
SA	–0.10 (–0.06)	**–0.42 (–0.40)**	–0.11 (–0.22)	0.10 (–0.08)	–0.20 (–0.01)	–0.03 (–0.28)	–0.15 (–0.16)
$\delta^{18}O$	0.00 (–0.22)	0.11 (–0.13)	–0.25 **(–0.41)**	**–0.44 (–0.42)**	**0.49 (0.39)**	–0.15 **(–0.41)**	–0.27 (–0.29)
d-excess	0.08 (0.01)	**0.79 (0.70)**	**0.37** (0.10)	–0.13 (–0.25)	**0.32 (0.52)**	–0.12 (–0.22)	**0.47** (0.27)

Table 7. Pearson's correlation coefficients (r) between the GV7-C ice core records and the climate variables for the period 1872–2013 CE. Correlations are calculated for annual data, running averages, and three- and five-year averages (shown in parentheses). Larger values ($r > 0.3$ at $p < 0.05$) are marked in underlined bold.

	IOD	SST (SEIO)	SST anomaly	SAM	Niño3.4
			Annual		
SA	0.10	–0.11	–0.01	0.03	0.02
$\delta^{18}O$	–0.04	–0.02	–0.08	–0.14	0.13
d-excess	–0.04	–0.02	–0.08	–0.14	0.13
			3-yr running average (three-year average)		
SA	0.01 (–0.07)	0.02 (–0.01)	0.02 (–0.06)	0.09 (–0.02)	0.03 (0.07)
$\delta^{18}O$	–0.11 (–0.16)	–0.02 (–0.17)	–0.11 (–0.20)	–0.16 (–0.19)	0.18 (0.18)
d-excess	0.23 (0.29)	**0.43 (0.41)**	**0.39 (0.40)**	0.24 (0.25)	0.26 (0.35)
			5-yr running average (five-year average)		
SA	–0.04 (–0.09)	0.11 (0.16)	0.04 (0.14)	0.07 (0.18)	0.15 (–0.03)
$\delta^{18}O$	–0.09 (–0.05)	–0.03 (–0.05)	–0.11 (–0.03)	–0.14 (–0.05)	0.12 (0.07)
d-excess	**0.30 (0.73)**	**0.46 (0.78)**	**0.43 (0.76)**	**0.30 (0.71)**	0.16 (0.36)

Line 347: Please consider adding the word “partly” to “…(decreasing) d18O can be _____ explained by the intrusion…”.

Answer: Thank you for the comment, we have edited accordingly.

3.4 Discussion and implications

The variations in SA data from the GV7-C ice core show no obvious trend and are not correlated to climate drivers examined in this study. The SA of the GV7-C ice core is assumed to be affected by the coupled influence of dynamic processes (i.e., the transport pathways and transport efficiency of moist air) or abrupt synoptic events (e.g., intense transport by atmospheric river events). The variability in SA is affected by moisture transport via large-scale atmospheric circulation (Thomas et al., 2008; Udy et al., 2021; Cohen et al., 2012) and synoptic-scale short-lived events (e.g., atmospheric river events, atmospheric rivers) (Turner et al., 2019; Wille et al., 2021) and evident in the ice core records from coastal regions (Servettaz et al., 2020; Jackson et al., 2023). Moreover, the intensity and frequency of cyclone events also affect snowfall in Antarctic coastal areas (Dalaiden et al., 2020a). Particularly, in the Ross Sea region, the cyclonically driven SA is dominant and the region is sensitive to tropical and local climate drivers (Bertler et al., 2018). The contribution of synoptic-scale transport has been reported to be large for Victoria Land based on simulations over the 1985–2014 period (Dalaiden et al., 2020a). The influence of the ENSO on SA was evident at the Law Dome site (Roberts et al., 2015).

Based on the correlation of $\delta^{18}O$ in the GV7-C ice core with Nino 3.4, SOI, SAM, and SIE over the Ross-Amundsen Sea sector for 1957–2013 CE, the increasing (decreasing) $\delta^{18}O$ can be partly explained by the intrusion of relatively warm (colder) and moist (dry) air mass mainly through the PO sector of the Southern Ocean. This finding is comparable to other ice cores from the coastal Antarctica. In the Aurora Basin North ice core from East Antarctica, a weak negative correlation ($r = -0.24$) was observed between the SAM and $\delta^{18}O$ for 2005–2014 CE (Servettaz et al., 2020). This suggests a negative phase of the SAM

Line 349-350: A correlation is reported over the period 2005-2014 CE. Is this correlation (R=-0.24) statistically significant? If not, please remove it from the manuscript and report that “no statistically significant correlations were found” in that core over that period of time.

Line 351-353: Please add a reference to that line.

Answer: Thank you for this very helpful comments. We double checked and excluded it.

3.4 Discussion and implications

The variations in SA data from the GV7-C ice core show no obvious trend and are not correlated to climate drivers examined in this study. The SA of the GV7-C ice core is assumed to be affected by the coupled influence of dynamic processes (i.e., the transport pathways and transport efficiency of moist air) or abrupt synoptic events (e.g., intense transport by atmospheric river events). The variability in SA is affected by moisture transport via large-scale atmospheric circulation (Thomas et al., 2008; Udy et al., 2021; Cohen et al., 2012) and synoptic-scale short-lived events (e.g., atmospheric river events, atmospheric rivers) (Turner et al., 2019; Wille et al., 2021) and evident in the ice core records from coastal regions (Servettaz et al., 2020; Jackson et al., 2023). Moreover, the intensity and frequency of cyclone events also affect snowfall in Antarctic coastal areas (Dalaiden et al., 2020a). Particularly, in the Ross Sea region, the cyclonically driven SA is dominant and the region is sensitive to tropical and local climate drivers (Bertler et al., 2018). The contribution of synoptic-scale transport has been reported to be large for Victoria Land based on simulations over the 1985–2014 period (Dalaiden et al., 2020a). The influence of the ENSO on SA was evident at the Law Dome site (Roberts et al., 2015).

Based on the correlation of $\delta^{18}O$ in the GV7-C ice core with Nino 3.4, SOI, SAM, and SIE over the Ross-Amundsen Sea sector for 1957–2013 CE, the increasing (decreasing) $\delta^{18}O$ can be partly explained by the intrusion of relatively warm (colder) and moist (dry) air mass mainly through the PO sector of the Southern Ocean. This finding is comparable to other ice cores from the coastal Antarctica. In the Mount Brown South ice core in East Antarctica, evidence for moisture transport from the southern IO has been detectable from $\delta^{18}O$ signal, and the extreme precipitation events are linked with high-pressure systems in the mid-latitudes which increase the transport of warm and moist air mass from the southern IO (Jackson et al., 2023). In another ice core from Adélie Land covering the 1946–2006 CE period, decadal variations in $\delta^{18}O$ and regional temperature were correlated (Goursaud et al., 2017). Moreover, $\delta^{18}O$ shows a tendency to decrease with increasing wind speed. However, the $\delta^{18}O$ on an annual scale could not be explained by changes in the SIE and temperature, indicating the importance of site-dependent climate signals in coastal ice cores (Goursaud et al., 2017). In another study, isotope-based results indicated colder SSTs, a higher SIE, stronger katabatic winds, and decreasing SA in the Victoria Low Glacier ice core during the 1288–1807 period (the Little Ice Age period) (Bertler et al., 2011). Little Ice Age-related cooling is also evident in the $\delta^{18}O$ signal from the Hercules Neve ice core for the 1770–1890 period (Stenni et al., 1999) and frequent cold intervals in the Talos Dome ice core (Stenni et al., 2002). In line with these observations, a slight decreasing trend was observed in the $\delta^{18}O$ signal from the GV7-C ice core during the 1782–1845 CE period (Fig. 4), which may be part of Little Ice Age cooling. After 1845, there was

Line 369: Please correct “is contrast” for “contrasts”

Answer: Thank you for the comment, we have edited accordingly.

370 GV7-C ice core during the 1782–1845 CE period (Fig. 4), which may be part of Little Ice Age cooling. After 1845, there was no long-term trend in $\delta^{18}O$ from the GV7-C ice core; rather, values lower than the long-term mean were frequently observed (the blue lines in Fig. 4). This depletion of $\delta^{18}O$ observed from the GV7-C ice core may be possibly linked with changes in atmospheric circulation (e.g., SAM-related cooling) (Thompson and Solomon, 2002). Moreover, in terms of temperature reconstruction, $\delta^{18}O$ signal in the GV7-C ice core contrasts to anthropogenic global warming, suggesting more local/regional
375 variations or various climatic factors.

Lines 372-373: The sentence in these lines reports Southern Ocean warming co-varying with dexcess during 1991-2000 CE. While this statement may support the authors point, it also raises questions about the co-variability of these parameters outside those 10 years. Please, add more information about the Southern Ocean warming vs d-excess relationship outside that 10 year window.

Answer: Thank you for the comment, we meant here to elaborate the relationship (positive) between d-excess and SST. We then excluded the 1991-2000 CE period.

Based on the correlation of *d*-excess with SST-SEIO and SST anomaly (Table 4 and 7), the *d*-excess signal from the GV7-C ice core likely to preserve the thermodynamic changes (i.e., SST changes) particularly over the IO sector of the Southern Ocean. Notably, the southern Indian Ocean exhibits the most intense cyclonic activity in the Southern Ocean, which may enhance the detectability of this signal in the *d*-excess record (Simmonds et al. 2003). *D*-excess as an indicator of climate conditions in the source region (Jouzel et al., 1982; Sodemann and Stohl, 2009, Lewis et al., 2013), warming over the Southern Ocean, was found to co-vary with higher *d*-excess in the Victoria Lower Glacier ice core (Bertler et al., 2011). At the Law Dome ice core site, *d*-excess also reflects SST changes over the southern IO sector (Masson-Delmotte et al., 2003). Particularly the abrupt increase in the *d*-excess in the 1970s was consistent with the *d*-excess of the GV7-C ice core. This relevance was explained by the abrupt changes in meridional atmospheric circulation, which led to the intrusion of warm subtropical moisture sources to the Antarctic coast during the 1970s (Masson-Delmotte et al., 2003). Changes in the SAM have also been linked to

Line 375: The line states "… was consistent with the GV7-C ice core result". Please specify to which result you are referring to.

Answer: Thank you for the comment, we have edited accordingly.

Based on the correlation of *d*-excess with SST-SEIO and SST anomaly (Table 4 and 7), the *d*-excess signal from the GV7-C ice core likely to preserve the thermodynamic changes (i.e., SST changes) particularly over the IO sector of the Southern Ocean. Notably, the southern Indian Ocean exhibits the most intense cyclonic activity in the Southern Ocean, which may enhance the detectability of this signal in the *d*-excess record (Simmonds et al. 2003). *D*-excess as an indicator of climate conditions in the source region (Jouzel et al., 1982; Sodemann and Stohl, 2009, Lewis et al., 2013), warming over the Southern Ocean, was found to co-vary with higher *d*-excess in the Victoria Lower Glacier ice core (Bertler et al., 2011). At the Law Dome ice core site, *d*-excess also reflects SST changes over the southern IO sector (Masson-Delmotte et al., 2003). Particularly the abrupt increase in the *d*-excess in the 1970s was consistent with the *d*-excess of the GV7-C ice core. This relevance was explained by the abrupt changes in meridional atmospheric circulation, which led to the intrusion of warm subtropical moisture

Lines 389-390: Please check this sentence for clarity

Answer: Thank you for the comment, we have edited accordingly.

Based on various correlation analysis with the climate variables used in this study, the following interpretations are summarized. During the period 1957–2013 CE, the correlation patterns based on $\delta^{18}O$ and *d*-excess support that snow precipitating at the GV7-C site mainly originates from the Southern Ocean possibly via western PO and southeastern Indian Ocean. For the longer time scale (1872–2013), the correlation patterns based on *d*-excess for SST indicates air mass intrusion from the Indian Ocean sector of the Southern Ocean. This suggests a warmer (colder) ocean surface condition would be preserved in higher (lower) $\delta^{18}O$ (recent period) and *d*-excess values (recent and longer period) in the GV7-C ice core.

Lines 396-397: Please add a reference to this line.

Answer: Thank you for the comment, we have added.

3.4 Discussion and implications

The variations in SA data from the GV7-C ice core show no obvious trend and are not correlated to climate drivers examined in this study. The SA of the GV7-C ice core is assumed to be affected by the coupled influence of dynamic processes (i.e., the transport pathways and transport efficiency of moist air) or abrupt synoptic events (e.g., intense transport by atmospheric river events) (Turner et al., 2019; Wille et al., 2021). The variability in SA is affected by moisture transport via large-scale atmospheric circulation (Thomas et al., 2008; Udy et al., 2021; Cohen et al., 2012) and synoptic-scale short-lived events (e.g., atmospheric river events, atmospheric rivers) (Turner et al., 2019; Wille et al., 2021) and evident in the ice core records from coastal regions (Servettaz et al., 2020; Jackson et al., 2023). Moreover, the intensity and frequency of cyclone events also affect snowfall in Antarctic coastal areas (Dalaiden et al., 2020a). Particularly, in the Ross Sea region, the cyclonically driven

Line 411: The line states “It is useful…”. Please specify “what is useful” or reassess the sentence for clarity.

Citation: https://doi.org/10.5194/egusphere-2025-2408-RC2

Answer: Thank you for the comment, we have edited this paragraph which quite wordy and ambiguous.

Lastly, it is notable that the importance of the GV7-C ice core records in climate studies. The historical temperature variability over the tropical ocean is important for global warming scenarios (IPCC, 2019). The projections show oceanic and atmospheric warming (Timmermann and Hellmer, 2013), and heat transported by the Southern Ocean further induces the melting of Antarctic ice shelves (Rignot et al., 2019). Particularly, the IO is experiencing the strongest and most robust warming (Du and Xie, 2008; Beal et al., 2019), largely driven by anthropogenic forcing (Dong et al., 2014), and it is projected to warm non-uniformly (Sharma et al., 2023). The IO and the PO temperature anomaly affects the surface air temperature of Antarctica (Zhang and Duan, 2023). Moreover, warm SSTs in the western tropical IO excite a poleward-moving Rossby wave, inducing the changes in sea ice extent (Zhang et al., 2024). The coastal and inland Antarctic regions emerge an anomalous retreat of sea ice extent and warming due to the short-term significant intrusion of warm and moist air masses associated with strong negative phase of SAM (Ionita et al., 2018). The SAM variation in the recent period is unprecedented in the last millennia (Fogt and Marshall, 2020) and the increasing influence of the SAM-ENSO coupling has been reported since the 1940s (in coastal Dronning Maud Land) (Ejaz et al., 2022). Thus, understanding the response of the Antarctic climate to ocean variability of the IO sector would be important. Although, taking into account all possible influences was not feasible and would be beyond the scope of this study; nevertheless, the results may be useful for further research on the influence of atmospheric circulation, transport efficiency, and abrupt synoptic events in more details.

We appreciate all comments and suggestions on our manuscript. We are looking forward to its publication. Thank you for handling our manuscript and your patience.

Sincerely,
Jeonghoon Lee